"W-X-M" transformations in isomerization of B39− borospherenes

Ting-Ting Gao, Qiang Chen, Yue-Wen Mu, Haigang Lu, and Si-Dian Li

Citation: AIP Advances **6**, 065110 (2016); doi: 10.1063/1.4954030
View online: http://dx.doi.org/10.1063/1.4954030
View Table of Contents: http://scitation.aip.org/content/aip/journal/adva/6/6?ver=pdfcov
Published by the AIP Publishing

"W-X-M" transformations in isomerization of B_{39}^- borospherenes

Ting-Ting Gao, Qiang Chen, Yue-Wen Mu, Haigang Lu,[a] and Si-Dian Li[a]
Key Laboratory of Materials for Energy Conversion and Storage of Shanxi Province, Institute of Molecular Science, Shanxi University, Taiyuan 030006, P. R. China

(Received 29 February 2016; accepted 2 June 2016; published online 10 June 2016)

The Stone-Wales transformation plays an important role in the isomerization of fullerenes and graphenic systems. The continuous conversions between neighboring six- and seven-membered rings in the borospherene (all-boron fullerene) B_{40} had been discovered (Martínez-Guajardo *et al*. Sci. Rep. **5**, 11287 (2015)). In the first axially chiral borospherenes C_3 B_{39}^- and C_2 B_{39}^-, we identify three active boron atoms which are located at the center of three alternative sites involving five boron atoms denoted as "W", "X", and "M", respectively. The concerted movements of these active boron atoms and their close neighbors between neighboring six- and seven-membered rings define the "W-X-M" transformation of borospherenes. Extensive first-principles molecular dynamics simulations and quadratic synchronous transit transition-state searches indicate that, via three transition states (TS1, TS2, and TS3) and two intermediate species (M1 and M2), the three-step "W-X-M" transformations convert the C_3 B_{39}^- global minimum into its C_2 isomer at room temperature (300 K) and vice versa. The maximum barriers are only 3.89 kcal/mol from C_3 to C_2 B_{39}^- and 2.1 kcal/mol from C_2 to C_3 B_{39}^-, rendering dynamic fluxionalities to these borospherenes. Therefore, the "W-X-M" transformation plays an important role in the borospherenes and borospherene-based nanostructures.
[http://dx.doi.org/10.1063/1.4954030]

I. INTRODUCTION

Shortly after the discovery of fullerenes,[1] the Stone-Wales transformation was proposed as a possible mechanism for interconversion between fullerene isomers.[2] By rotating a C-C bond by 90° with regard to the midpoint of the bond, the Stone-Wales transformation makes four hexagons turn into two pentagons and two heptagons. In particular, this transformation has the lowest formation energy in the isomerization of fullerenes and graphenic systems.[3–9]

The first all-boron fullerene D_{2d} $B_{40}^{-/0}$, referred to as borospherene in literature, was discovered in 2014 in a combined experimental and theoretical investigation,[10] and leads to a quick surge of borospherene chemistry, an area parallel to carbon fullerene chemistry.[11–18] The first axially chiral borospherenes, C_3 and C_2 B_{39}^-, were observed in 2015.[19] Recently, three chiral B_{41}^+, B_{42}^{2+}, and B_{44} cages were predicted using the extensive global-minimum searches and the first principle calculations.[20,21] All of these borospherenes are cubic-like in geometric structures which are composed of twelve interwoven boron double-chains (BDCs) with six B_6 hexagons, B_7 heptagons, and/or B_9 nonagons on the faces.

Because of the electron deficiency of boron, there exist extensive multicenter B-B bonds in boron sheets and cages,[10,19,22–26] making their geometric structures fluxional. The structural fluxionality of small boron clusters has been widely investigated to design nano-devices.[18,27–32] For instance, a series of Wankel motor molecules including B_{11}^-, B_{13}^+, B_{18}^{2-}, and B_{19}^- were discovered using the

[a]Authors to whom correspondence should be addressed. Electronic addresses: luhg@sxu.edu.cn; lisidian@sxu.edu.cn.

first-principles methods.[28–32] In particular, first-principles molecular dynamics (FPMD) simulations demonstrated that the structural transformation of B_5 fragment between six- and seven-membered rings is an element process in isomerization of the B_{40} fullerene.[18]

The axially chiral B_{39}^- fullerenes possess a distinctive structural fluxionality: B_{39}^- hops between the C_3 and C_2 isomers with low energy barriers during FPMD simulations at 300K. In the two close-lying isomers, C_2 B_{39}^- is the first borospherene observed with a tetracoordinate boron atom at the "defect" site of a boron double chain.[19] B_{39}^- therefore may serve as a preferred model to investigate the structural transformations and isomerization of borospherenes.

We carefully investigated the structural characteristics of the B_{39}^- fullerenes and found that both the C_3 and C_2 B_{39}^- fullerenes can be viewed as the combinations of a spherical B_{36} skeleton with three active boron atoms on the BDCs between neighboring hexagonal and heptagonal holes. The concerted movements of these active born atoms and their directly bonded neighbors make the B_{39}^- fullerene fluctuate between its low-lying isomers at room temperature.

II. COMPUTATIONAL METHODS

The geometric structures of all B_{39}^- fullerenes were optimized at the CAM-B3LYP/6-311+G* and PBE0/6-311+G* levels, respectively.[33–38] Both of their single point energies were calculated at the CCSD(T)/6-31G* level[39–42] using the Molpro2012 package.[43] Though the optimized geometric structures of these borospherenes have only some negligible difference between the CAM-B3LYP and PBE0 functionals, the relative energies of CAM-B3LYP are more approximate to those of CCSD(T) than those of PBE0.[19] Therefore, the CAM-B3LYP functional was chosen to investigate the other properties of borospherenes. The transition states (TS) were searched using the quadratic synchronous transit (QST) approach[44,45] at the CAM-B3LYP/6-31G* levels. To confirm the connectivity of minima and saddle points, the intrinsic reaction coordinates were scanned with the step size of 0.05 Bohr on both directions. All of these first principle calculations, except the CCSD(T) ones, were carried out using Gaussian 09 package.[46]

The FPMD simulations of the B_{39}^- fullerenes were performed using the QUICKSTEP module of CP2K2.6 suite[47] at the temperatures of 200, 300, and 500K, respectively. The electronic part of calculations is handled with the BLYP functional[48,36] employing a mixed Gaussian and plane waves approach. The Gaussian basis set is double-zeta valence polarization basis set with Goedecker–Teter–Hutter pseudopotentials,[49] and the energy cutoff for plane waves is 280 Rydbergs. The simulations are launched from the optimized geometry of C_2 or C_3 B_{39}^- fullerenes in a 1.5nm cubic box with random velocities assigned to the atoms, employing a Hoover thermal bath,[50,51] for a simulation time of 30 ps with 1.0 fs time steps. All B-B bond lengths above and under the active boron atoms were monitored along the trajectories to determine the sites of active boron atoms in the simulations.

III. RESULTS AND DISCUSSION

It had been observed that the B_{39}^- borospherenes have a C_3 cage global minimum with a close-lying C_2 cage isomer (Fig. 1(A) and 1(D)), both of which consist of a similar spherical B_{36} skeleton and three active boron atoms on the BDCs at the waist. In the C_3 cage, all the three active boron atoms lie at the center of three upper sites mainly involving five boron atoms (denoted as "W", Fig. 1(A)), while in the C_2 cage the three active boron atoms are located at the center of the lower ("M"), middle ("X"), and upper sites involving three B_5 units, respectively (Fig. 1(D)). Thus, each active boron atom in B_{39}^- has three possible locations to occupy, at the center of either W, X, or M sites (Fig. 1).

Because the spherical B_{36} skeleton, a new type of three-chain boron cage,[52] is relatively inactive, it can be used to construct a family of B_{39}^- cages with three active boron atoms at its waist. Obviously, there are $3^3 = 27$ combinations of the "W", "X", and "M" active boron atoms in this B_{39}^- family, whose specific geometric structures can be systemically denoted by three occupied sites of

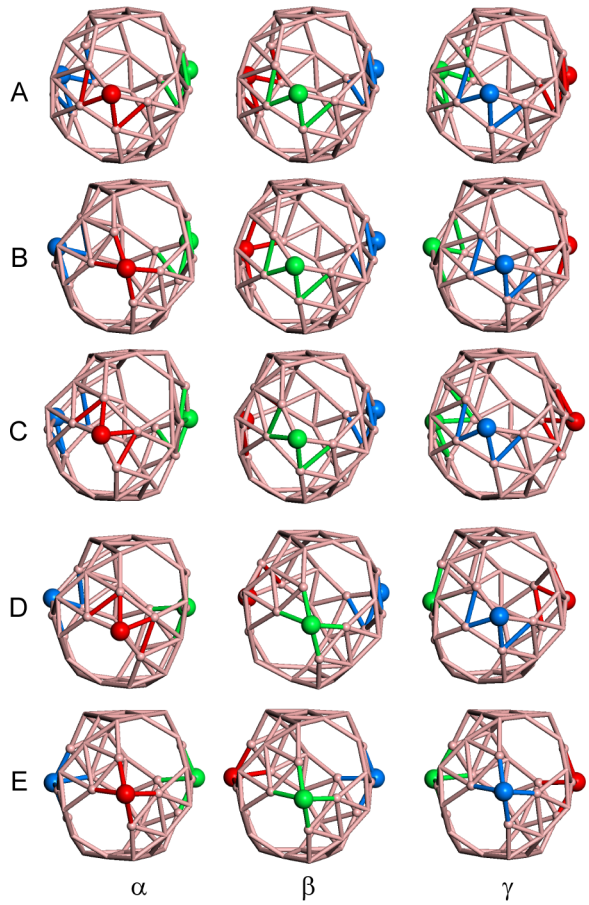

FIG. 1. Typical geometric structures of the B_{39}^- fullerenes: (A) C_3, (B) M_1, (C) M_2, (D) C_2, and (E) D_3. The α, β, and γ are their front, right-back, and left-back views, and the red, green, and blue balls indicate three active boron atoms at the waist, respectively.

active boron atoms (TABLE I). For instance, the C_3 and C_2 B_{39}^- fullerenes have the "WWW" and "MXW" structures (Fig. 1(A) and 1(D)), respectively.

In this family, all 27 B_{39}^- cages are classified into six nonequivalent groups: D_3, C_3, C_2, M_1, M_2, and M_3, which include 1, 2, 6, 6, 6, and 6 specific geometric structures, respectively (TABLE I). The high symmetry D_3 "XXX" B_{39}^- fullerene should be taken as the primitive cage of the B_{39}^- family: its distortions will produce all other isomers with C_3, C_2, or C_1 symmetries. The M_3 isomers

TABLE I. Specific geometric structures and relative energies (kcal/mol) of the B_{39}^- fullerenes.

Name	Symmetry	Geometric structures	$E_{CAM-B3LYP}$	E_{PBE0}	$E_{CCSD(T)//CAM-B3LYP}$	$E_{CCSD(T)//PBE0}$
D_3	D_3	XXX	4.62	7.04	4.64	10.31
C_3	C_3	WWW	0.00	0.00	0.00	0.00
		MMM				
M_1	C_1	XWW, WXW, WWX	2.84	4.57	3.78	3.97
		XMM, MXM, MMX				
M_2	C_1	MWW, WMW, WWM	2.68	4.67	3.98	3.90
		WMM, MWM, MMW				
C_2	C_2	MXW, WMX, XWM	0.73	3.07	1.74	2.20
		WXM, MWX, XMW				
M_3	-	XXW, XWX, WXX	-	-	-	-
		XXM, XMX, MXX				

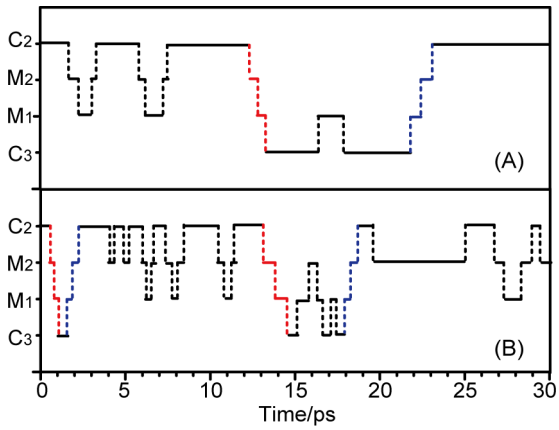

FIG. 2. Presences (horizontal solid lines) and transformations (vertical dashed lines) of C_3, M_1, M_2, and C_2 B_{39}^- fullerenes at 300K (A) and 500K (B).

are not true local minima. The energies of the D_3, M_1, and M_2 isomers are only 4.64, 3.78, and 3.98 kcal/mol less stable than the global minimum C_3 cage at the CCSD(T)/6-31G* level. These newly predicted species are expected to coexist with the observed C_3 and C_2 isomers in experiments under certain conditions (TABLE I), although they were not identified in the previously reported photoelectron spectroscopy (PES) of B_{39}^- which is rather congested and may contain contributions from other isomers.[19]

To locate all possible coexisting borospherenes, extensive FPMD simulations of the C_2 and C_3 B_{39}^- fullerenes were performed at 200, 300, and 500K, respectively.[19,53] At 200K, both of the C_2 and C_3 B_{39}^- fullerenes are stable and cannot be converted into the other low-lying isomers. However, at 300K and especially 500K, the C_3, C_2, M_1, and M_2 B_{39}^- isomers all coexist in the FPMD simulations of B_{39}^-, except the D_3 one with an XXX sequence (Fig. 2).

In the FPMD simulations at 300K and 500K, there exist three-step reversible structural transformations among the C_3, C_2, M_1, and M_2 B_{39}^- isomers (FIG. 2): from C_3 to M_1 (FIG. 1(Aα) and 1(Bα)), from M_1 to M_2 (Fig. 1(Bα) and 1(Cα)), and from M_2 to C_2 (Fig. 1(Cβ) and 1(Dβ)). All of these transformations originate from the movements of three active boron atoms between different sites. For an active boron atom, its "W-X" transformation expands the lower hexagon into a heptagon by breaking a B-B bond under it, and its "X-M" transformation shrinks the upper heptagon into a hexagon by forming another B-B bond above it (Fig. 3), which was firstly discovered in isomerization of the B_{40} fullerene.[18] Obviously, an active boron atom has only two elementary transformations: "W-X" and "X-M". Here, the "W-X-M" transformation is used to denote all elementary transformations and their various combinations of active boron atoms. Such an mechanism can be easily extended to other borospherenes involving octagonal and nanogonal rings etc, depending on the specific geometries of the systems.[20,21]

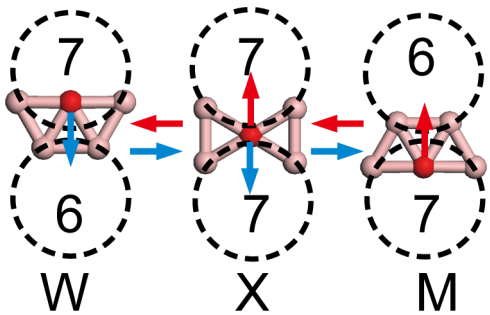

FIG. 3. "W-X-M" transformation between neighboring hexagon (6) and heptagon (**7**). The blue and red arrows denote the forward and backward "W-X-M" transformation, respectively.

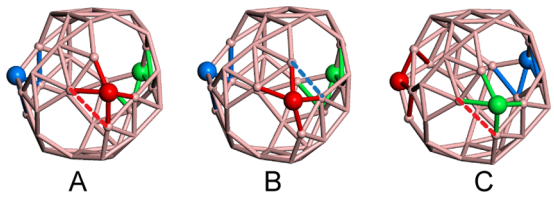

FIG. 4. Typical geometric structures of three transition states in the isomerization between the C_3 and C_2 B_{39}^- fullerenes: (A). TS_1 (between C_3 and M_1), (B) TS_2 (between M_1 and M_2), and (C) TS_3 (between M_2 and C_2). The red, blue, and green balls indicate three active boron atoms, and the red and blue dashed lines indicate the broken and forming B-B bonds in the reactions, respectively.

In the FPMD simulations at 300 and 500K, the isomerization from the global minimum C_3 cage to its close-lying C_2 isomers (blue and red lines in Fig. 2) includes the "W-X" and "X-M" transformations of an active boron atom, and the "W-X" transformation of another active boron atom. Furthermore, the isomerization between the C_3 "WWW" and "MMM" structures can also occur by three successive "W-X-M" transformations of three active boron atoms: C_3(WWW) → M_1(XWW) → M_2(MWW) → C_2(MXW) → M_2(MMW) → M_1(MMX) → C_3(MMM). In addition, there are also many incomplete isomerization processes, such as the C_2-M_2-C_2, C_3-M_1 – C_3, and C_3-M_1-M_2-M_1-C_3 transformations.

Beside the B_{39}^- borospherenes, there is the similar "W-X-M" transformation between the six- and seven-membered rings of B_{40} borospherene in the FPMD simulations at high temperature (1200K).[13] Therefore, the "W-X-M" transformation plays an important role in the isomerization of borospherenes, just as the role of Stones-Wales transformation in the fullerenes and graphenic systems. However, in contrast with the C-C bond rotation in Stones-Wales transformation, the "W-X-M" transformation originates from the movement of some active boron atoms. In addition, because of the axial chirality of these B_{39}^- fullerenes, there is another family of degenerate enantiomers, in which the "W-X-M" transformations can also occur in their isomerization.

The most important isomerization is the reaction between the C_3 and C_2 B_{39}^- fullerenes, whose transition states were found between C_3 and M_1 (TS_1), between M_1 and M_2 (TS_2), and between M_2 and C_2 (TS_3) (Fig. 4 and 5). The scans of their intrinsic reaction coordinates confirmed their reaction mechanisms.[54] Their small imaginary harmonic vibrational frequencies (TS_1: 104*i*, TS_2: 55*i*, and TS_3: 89*i* cm^{-1}) demonstrated that the structural transformations are moderate.

The energies of these transition states are 3.89, 3.60, and 2.84 kcal/mol with respect to the C_3 global minimum at the CAM-B3LYP/6-311+G* level, respectively. Then their barriers from C_3 to C_2 isomers are 3.89, 0.76, and 0.16 kcal/mol so that the C_3 to M_1 transformation is the rate determining step. The maximum barrier of 3.89 kcal/mol implies that the isomerization from C_3 to C_2 isomers could occur at the room temperature, just as shown in the FPMD simulation at 300K. Reversibly, the barriers from C_2 to C_3 isomers are 2.11, 0.92, and 1.05 kcal/mol at the

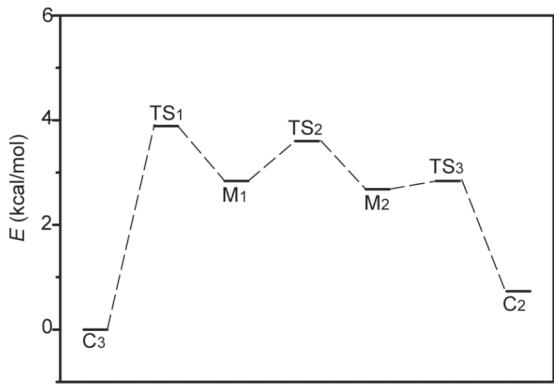

FIG. 5. Reaction pathway between the C_3 and C_2 B_{39}^- fullerenes.

CAM-B3LYP/6-311+G* level, respectively, which is much lower than the maximum barrier (3.89 kcal/mol). Therefore, the isomerization from C_2 to C_3 isomers is easier than that from C_3 to C_2 isomers.

The maximum isomerization barrier (3.89kcal/mol) of B_{39}^- fullerenes is much lower than that of the Stone-Wales transformation in carbon materials (162.9 kcal/mol at the B3LYP/6-311G* level).[3] Obviously, the isomerization of B_{39}^- boron fullerenes are easier than that of carbon fullerenes. Furthermore, this barrier is also lower than that of isomerization (14.3kcal/mol) in the B_{40} fullerene.[18] Compared with the one-step isomerization of the B_{40} fullerene, there are three-step successive "W-X-M" transformations between two coexisting C_3 and C_2 B_{39}^- isomers. Therefore many B_{39}^- cage isomers coexist at room temperature, which provides a reaction kinetic origin of the polymorphism of boron fullerenes.[53]

IV. CONCLUSIONS

Based on the structural characteristic of C_3 and C_2 B_{39}^- boroshperenes, a family of B_{39}^- fullerenes were discovered, all of which consist of a spherical B_{36} skeleton and three active boron atoms. Each of the active boron atoms has three alternative sites (denoted as "W", "X", and "M"). All of the stable B_{39}^- fullerenes can coexist and transform each other at 300 and 500 K by the "W-X-M" transformations, which was firstly discovered in isomerization of the B_{40} fullerene. These "W-X-M" transformations play an important role in the isomerization of borospherenes, just as the Stone-Wales transformation in isomerization of carbon materials. In contrast with the C-C bond rotation in Stones-Wales transformation, the "W-X-M" transformation originates from the movement of some active boron atoms. The maximum barrier is only 3.89 kcal/mol from the C_3 to C_2 B_{39}^- fullerenes so that they can transform each other easily at room temperature. This finding reveals the dynamic characteristic of borospherenes and can be used to design the new borospherene-based materials.

ACKNOWLEDGEMENTS

This work was supported by the NSFC (Grants No. 21373130, 21473106, and 11504213). We also thank the High-Performance Computing Platform of Shanxi University for funding the computer time.

[1] H. W. Kroto, J. R. Heath, S. C. O'Brien, R. F. Curl, and R. E. Smalley, Nature **318**, 162 (1985).
[2] A. J. Stone and D. J. Wales, Chem. Phys. Lett. **128**, 501 (1986).
[3] H. F. Bettinger, B. I. Yakobson, and G. E. Scuseria, J. Am. Chem. Soc. **125**, 5572 (2003).
[4] P. W. Dunk, N. K. Kaiser, C. L. Hendrickson, J. P. Quinn, C. P. Ewels, Y. Nakanishi, Y. Sasaki, H. Shinohara, A. G. Marshall, and H. W. Kroto, Nat. Chem. **3**, 855 (2012).
[5] I. N. Ioffe, A. A. Goryunkov, N. B. Tamm, L. N. Sidorov, E. Kemnitz, and S. I. Troyanov, Angew. Chem. Int. Ed. **121**, 6018 (2009).
[6] G. D. Lee, E. Yoon, K. He, A. W. Robertson, and J. H. Warner, Nanoscale **6**, 14836 (2014).
[7] A. J. M. Nascimento and R. W. Nunes, Nanotechnology **24**, 435707 (2013).
[8] Z. A. Zhang, A. Kutana, and B. I. Yakobson, Nanoscale **7**, 2716 (2015).
[9] S. T. Skowron, I. V. Lebedeva, A. M. Popov, and E. Bichoutskaia, Chem. Soc. Rev. **44**, 3143 (2015).
[10] H. J. Zhai, Y. F. Zhao, W. L. Li, Q. Chen, H. Bai, H. S. Hu, Z. A. Piazza, W. J. Tian, H. G. Lu, Y. B. Wu, Y. W. Mu, G. F. Wei, Z. P. Liu, J. Li, S. D. Li, and L. S. Wang, Nat. Chem. **6**, 727 (2014).
[11] H. Bai, Q. Chen, H. J. Zhai, and S. D. Li, Angew. Chem. Int. Ed. **54**, 941 (2015).
[12] R. X. He and X. C Zeng, Chem. Commun. **51**, 3185 (2015).
[13] H. L. Dong, T. J. Hou, S. T. Lee, and Y. Y. Li, Sci. Rep. **5**, 09952 (2015).
[14] G. P. Gao, F. X. Ma, Y. L. Jiao, Q. Sun, Y. Jiao, E. Waclawik, and A. J. Du, Comput. Mater. Sci. **108**, 38 (2015).
[15] H. L. Dong, B. Lin, K. Gilmore, T. J. Hou, S. T. Lee, and Y. Y. Li, Curr. Appl. Phys. **15**, 1084 (2015).
[16] Z. Yang, Y. L. Ji, G. Q. Lan, L. C. Xu, X. G. Liu, and B. S. Xu, Solid State Commun. **217**, 38 (2015).
[17] W. Fa, S. Chen, S. Pande, and X. C. Zeng, J. Phys. Chem. A **119**, 11208 (2015).
[18] G. M. Guajardo, J. L. Cabellos, A. D. Celaya, S. Pan, R. Islas, P. K. Chattaraj, T. Heine, and G. Merino, Sci. Rep. **5**, 11287 (2015).
[19] Q. Chen, W. L. Li, Y. F. Zhao, S. Y. Zhang, H. S. Hu, H. R. Li, W. J. Tian, H. G. Lu, J. Li, and L. S. Wang, ACS Nano. **9**, 754 (2015).
[20] Q. Chen, S. Y. Zhang, H. Bai, W. J. Tian, T. Gao, H. R. Li, C. Q. Miao, Y. W. Mu, H. G. Lu, H. J. Zhai, and S. D. Li, Angew. Chem. Int. Ed. **54**, 8160 (2015).

[21] T. B. Tai and M. T. Nguyen, Chem. Commun. (2015); DOI: 10.1039/c5cc09111j.
[22] A. P. Sergeeva, I. A. Popov, Z. A. Piazza, W. L. Li, C. Romanescu, L. S. Wang, and A. I. Boldyrev, Acc. Chem. Res. **47**, 1349 (2014).
[23] W. Huang, A. P. Sergeeva, H. J. Zhai, B. B. Averkiev, L. S. Wang, and A. I. Boldyrev, Nat. Chem. **2**, 202 (2010).
[24] J. J. Zhao, X. M. Huang, R. L. Shi, H. S. Liu, Y. Su, and R. B. King, Nanoscale **7**, 15086 (2015).
[25] L. Wang, J. J. Zhao, F. Y. Li, and Z. F. Chen, Chem. Phys. Lett. **501**, 16 (2010).
[26] N. G. Szwacki, A. Sadrzadeh, and B. I. Yakobson, Phys. Rev. Lett. **98**, 166804 (2007).
[27] S. Erhardt, G. Frenking, Z. F. Chen, and P. R. Schleyer, Angew. Chem. Int. Ed. **44**, 1078 (2005).
[28] Y. J. Wang, X. Y. Zhao, Q. Chen, H. J. Zhai, and S. D. Li, Nanoscale. **7**, 16054 (2015).
[29] J. Zhang, A. P. Sergeeva, M. Sparta, and A. N. Alexandrova, Angew. Chem. Int. Ed. **51**, 8512 (2012).
[30] D. Moreno, S. Pan, L. L. Zeonjuk, R. Islas, E. Osorio, G. Martínez-Guajardo, P. K. Chattaraj, T. Heine, and G. Merino, Chem. Commun. **50**, 8140 (2014).
[31] J. O. C. Jiménez-Halla, R. Islas, T. Heine, and G. Merino, Angew. Chem. Int. Ed. **49**, 5668 (2010).
[32] F. Cervantes-Navarro, G. Martínez-Guajardo, E. Osorio, D. Moreno, W. Tiznado, R. Islas, K. J. Donald, and G. Merino, Chem. Commun. **50**, 10680 (2014).
[33] R. Krishnan, J. S. Binkley, R. Seeger, and J. A. Pople, J. Chem. Phys. **72**, 650 (1980).
[34] G. D. Purvis and R. J. Bartlett, J. Chem. Phys. **76**, 1910 (1982).
[35] A. D. Becke, J. Chem. Phys. **98**, 5648 (1993).
[36] C. Lee, W. Yang, and R. G. Parr, Phys. Rev. B **37**, 785 (1988).
[37] T. Yanai, D. Tew, and N. Handy, Chem. Phys. Lett. **393**, 51–57 (2004).
[38] J. P. Perdew, K. Burke, and M. Ernzerhof, Phys. Rev. Lett. **77**, 3865 (1996).
[39] C. Adamo and V. Barone, J. Chem. Phys. **110**, 6158 (1999).
[40] J. Cizek, in *Adv. Chem. Phys.*, edited by P. C. Hariharan (Wiley Interscience, New York, 1969), Vol. 14, p. 35.
[41] G. E. Scuseria, C. L. Janssen, and H. F. Schaefer III, J. Chem. Phys. **89**, 7382.
[42] G. E. Scuseria and H. F. Schaefer III, J. Chem. Phys **90**, 3700 (1989).
[43] H. J. Werner *et al.*, MOLPRO, version 2012.1 (www.molpro.net).
[44] C. Peng and H. B. Schlegel, Israel J. Chem. **33**, 449 (1993).
[45] C. Peng, P. Y. Ayala, H. B. Schlegel, and M. J. Frisch, J. Comp. Chem. **17**, 49 (1996).
[46] M. J. Frisch *et al.*, Gaussian 09, revision A.2, Gaussian Inc., Wallingford, Connecticut, 2009.
[47] J. V. Vondele, M. Krack, F. Mohamed, M. Parrinello, T. Chassaing, and J. Hutter, Comput. Phys. Commun. **167**, 103 (2005).
[48] A. D. Becke, Phys. Rev. A **38**, 3098 (1988).
[49] S. Goedecker, M. Teter, and J. Hutter, Phys. Rev. B **54**, 1703 (1996).
[50] S. Nosé, J. Chem. Phys. **81**, 511 (1984).
[51] W. G. Hoover, Phys. Rev. A **31**, 1695 (1985).
[52] H. Lu and S.-D. Li, J. Chem. Phys. **138**, 114107 (2013).
[53] S. De, A. Willand, M. Amsler, P. Pochet, L. Genovese, and S. Goedecker, Phys. Rev. Lett. **106**, 225502 (2011).
[54] See supplementary material at http://dx.doi.org/10.1063/1.4954030 for the molecular dynamics simulations, reaction path, and geometric structures.